

Bridge Clogging in Belgium and Germany during the 2021 Floods

Daan Willem Poppema¹, Lisa Burghardt², Loïc Bénet³, Davide Wüthrich¹, Elena-Maria Klopries², Benjamin Dewals³, and Sebastien Erpicum³

¹Delft University of Technology

²Rheinisch Westfälische Technische Hochschule Aachen

³University of Liège

November 01, 2024

Abstract

In the summer of 2021, devastating river floods occurred in Western Europe as a result of extreme rainfall. At numerous bridges, debris accumulations were observed, exacerbating flooding upstream by impeding waterflow and sometimes contributing to bridge failure. Due to widespread building damage and flooding of settlements along the rivers, these accumulations differed markedly from classic logjams, with substantial amounts of man-made objects. A new database of clogged bridges in Belgium and Germany – described in a separate data descriptor – was analysed to characterise bridge clogging and determine the effect of bridge design, bridge location and hydraulic conditions. Nearly half of the debris volume consisted of man-made materials, including building rubble, anthropogenic wood and vehicles. This created remarkably dense accumulations, highlighting the importance of further studying debris accumulations of mixed composition. Examination of the relations between bridge design and accumulation volumes found bridges with narrow pier spacing ([?]10 metres) more susceptible to forming large accumulations. Blocking by the deck and railing also played a prominent role, in conjunction with blocking by the piers, as peak water levels at most bridges (85%) reached or exceeded the deck. These findings can help to better understand bridge clogging effects on flood conditions, to design bridges with lower debris accumulation risks, and to inform future flood hazard assessments, flood risk mapping, and disaster response strategies, especially in urbanised regions.

Hosted file

Bridge Clogging in Belgium and Germany during the 2021 Floods.docx available at <https://authorea.com/users/849345/articles/1236444-bridge-clogging-in-belgium-and-germany-during-the-2021-floods>

14 Abstract

15 In the summer of 2021, devastating river floods occurred in Western Europe as a result of extreme
16 rainfall. At numerous bridges, debris accumulations were observed, exacerbating flooding upstream
17 by impeding waterflow and sometimes contributing to bridge failure. Due to widespread building
18 damage and flooding of settlements along the rivers, these accumulations differed markedly from
19 classic logjams, with substantial amounts of man-made objects. A new database of clogged bridges in
20 Belgium and Germany – described in a separate data descriptor – was analysed to characterise bridge
21 clogging and determine the effect of bridge design, bridge location and hydraulic conditions. Nearly
22 half of the debris volume consisted of man-made materials, including building rubble, anthropogenic
23 wood and vehicles. This created remarkably dense accumulations, highlighting the importance of
24 further studying debris accumulations of mixed composition. Examination of the relations between
25 bridge design and accumulation volumes found bridges with narrow pier spacing (≤ 10 metres) more
26 susceptible to forming large accumulations. Blocking by the deck and railing also played a prominent
27 role, in conjunction with blocking by the piers, as peak water levels at most bridges (85%) reached or
28 exceeded the deck. These findings can help to better understand bridge clogging effects on flood
29 conditions, to design bridges with lower debris accumulation risks, and to inform future flood hazard
30 assessments, flood risk mapping, and disaster response strategies, especially in urbanised regions.

31 Plain language summary

32 In 2021, devastating river floods hit Western Europe. During these floods, floating debris built up in
33 front of many bridges. This increased flooding by partly blocking rivers and contributed to the failure
34 of bridges. Usually, accumulations mainly include trees, but this time they contained large amounts of
35 building rubble and man-made objects, from flooded and damaged buildings along the river. To study
36 this issue, we documented bridge clogging during the 2021 flood in Belgium and Germany in a
37 database. Analysis showed that about half of the documented debris was from man-made materials,
38 including building rubble, construction wood, cars and caravans. This resulted in remarkably dense
39 accumulations, with more flow resistance and a larger increase in upstream water levels. This
40 highlights that accumulations of mixed debris should be studied more in the future. The largest
41 accumulations happened at bridges with piers placed 10 metres or less apart. Debris blocking by the
42 deck and railing also played a prominent role, as most debris was blocked by flooded bridges, with a
43 submerged deck. These findings can help to design bridges with lower risk of debris blockages, and
44 inform disaster response strategies of where to expect debris accumulation during floods.

45

46 1. Introduction

47 During the summer of 2021, Western Europe experienced a catastrophic flood event, with rainfall of
48 150 mm to more than 250 mm within 48 hours in parts of Belgium, Germany, and neighbouring
49 countries (Journée et al., 2023; Mohr et al., 2023), which represents three months of averaged
50 precipitations within two days. The flood left a trail of devastation in its wake: destroying buildings,
51 roads, railways, bridges and other infrastructure (Wüthrich et al., 2024), creating more than 30 billion
52 euros of damages (Koks et al., 2021) and leading to at least 221 fatalities (Journée et al., 2023; Thieken
53 et al., 2023). In addition to the immense water discharges, the debris that was transported in the flow
54 caused substantial problems. Debris from destroyed infrastructure (rubbles) alongside with trees,
55 vehicles and other objects were carried away by the floodwaters and subsequently found in the
56 inundated areas. All this floating debris would often be blocked at bridges, creating debris
57 accumulations (see e.g. Figure 1) reducing the conveying capacity of an already overloaded water
58 infrastructure.

59 These debris accumulations can have devastating consequences on critical infrastructure, as well as
60 on the extent of the flood. They constrict bridge openings and obstruct the flow, leading to backwater
61 rise and increased inundation depths (De Cicco et al., 2018; Schalko et al., 2019; Schalko et al., 2018;
62 Schmocker & Hager, 2013). And crucially, most bridges are built in populated urban areas, so the
63 increased flooding occurs at locations where consequences can be enormous, both in terms of
64 damages as well as disruption to critical services. In addition, debris accumulations can contribute to
65 bridge failure, by increasing the forces acting on a bridge (Kimura et al., 2017; Oudenbroek et al., 2018;
66 Parola et al., 2000) or causing scour that undermines bridge foundations (Diehl, 1997; Lagasse et al.,
67 2010; Pagliara & Carnacina, 2011). As bridges are crucial infrastructure, such failure may have larger
68 consequences. During the 2021 flood, this became painfully clear in the Ahr valley in Germany, where
69 41 bridges were destroyed by the flood (Burghardt et al., 2024a), severely limiting emergency services
70 and disaster relief for cut-off settlements. These effects underline that debris clogging can play a
71 critical role in exacerbating flood impacts.

72 These processes highlight the critical need to understand and address the role of debris accumulation
73 during flood events. This subject has received quite some attention in the past, but most available
74 studies focus on accumulations consisting entirely of trees in mountain areas (see e.g. the reviews in
75 Comiti et al., 2016; De Cicco et al., 2018). Multiple studies also showed the critical role of debris during
76 coastal flooding, as large volumes of debris transported by tsunamis and storm surges can propagate
77 inland, causing supplementary forces and impulsive destruction (Chock et al., 2013; Robertson et al.,
78 2007; Saatcioglu et al., 2005; Takahashi et al., 2010; Wüthrich et al., 2020). Specifically for tsunamis,
79 Naito et al. (2014) provided a classification of potential debris, while studying its motion in coastal
80 areas and effects on the built environment. Results pointed out heterogeneous debris mixtures
81 containing shipping containers, vehicles (boats, vessels, cars), utility poles, dislodged buildings and

82 trees, if present along the coastline. Similarly, during the 2021 flood, the widespread flooding of more
83 urbanised areas brought vehicles, building rubble and many other objects into the debris
84 accumulations (Epicum et al., 2024b; Korswagen et al., 2022), in contrast to the previously studied
85 accumulations in mountain areas with more natural land use. This is also the reason why the term
86 *'floating debris'* is used throughout this paper. In contrast, for accumulations with only trees, 'large
87 wood accumulation' or 'logjam' are often preferred as more positive terms, in view of the ecological
88 benefits of deadwood in rivers (Ruiz-Villanueva et al., 2016; Wohl et al., 2016).



89

90 *Figure 1: A debris accumulation in Bad Neuenahr, Germany (bridge 16 in the database by Epicum et al. (2024)). Trees,*
91 *vehicles, tanks and other objects are present in front and on top of the bridge, with debris interlocking with the bridge*
92 *superstructure. Photo by Philipp von Ditfurth (Jannaschk, 2021).*

93 Observations suggest that the different shapes and materials of man-made objects compared to trees
94 change the accumulation process, flow resistance, backwater rise and interlocking with other debris
95 or bridge elements (see Figure 1, and Bayón et al., 2024; Burghardt et al., 2024b). However,
96 quantifying these effects requires systematic knowledge of the composition and characteristics of
97 these heterogeneous mixed debris accumulations, which is currently much more limited than for
98 natural debris accumulations (Table 1). Moreover, such a comprehensive understanding of the
99 mixture composition can support the development of realistic physical models to better reproduce
100 the hydraulic processes occurring during floods. In addition, analysis of the accumulations and the
101 main features of the bridges at which these occurred can help identifying how bridge design can be
102 optimised to decrease the probability of debris accumulation. This would be especially useful for
103 regions affected by the 2021 flood, where some bridges were destroyed and still need to be rebuilt,
104 but equally advantageous for future bridge design in general. Lastly, improved knowledge on the
105 accumulation characteristics and on the effect of bridge design will help to improve flood risk
106 assessments and damage estimations, in the mapping of future flood risks or in evacuation decisions
107 during floods.

Table 1: Debris composition measurements reported in literature

| Study | Flood event | Debris location | Debris contents |
|----------------------------|---------------------------------|---|--|
| Waldner et al. (2007) | Switzerland, 2005 | 40 driftwood accumulations, in Swiss streams and at lakes | On average 33% of the accumulation volume was deadwood (ranging from 12% to 55%), 58% fresh wood (ranging 15%-80%), 9% construction and firewood (ranging 5%-20%). Of the not yet cleaned-up accumulations, half of the volume consisted of pieces shorter than 7 m. For the full size distribution, see their Fig. 9.8. |
| Rickli et al. (2018) | None, regular conditions | In-stream large wood in 10 small Swiss mountain streams | By count, 6% of the large wood pieces consisted of entire trees, 20% snags with rootwads, 7% rootwads, 63% parts of logs, 4% parts of crowns. Half of the wood volume consisted of pieces shorter than 7 m. For the full size distribution, see their Fig. 3. |
| Bänziger (1990) | Switzerland, 1987 | Accumulations of 1700 m ³ total around Goms, Switzerland | 35% of the accumulation volume was deadwood, 48% fresh wood, 17% construction and firewood. The median log length (by piece count, not volume) was 4 m. For the full size distribution, see their Fig. 7. |
| Manners et al. (2007) | None: regular conditions | 3 bank accumulations at the Indian River (Hudson River watershed, USA) | On average, 69% of the accumulation volume was large wood (diameter>10 cm), 17% medium wood (1 cm<d<10 cm), 5% small wood (d<1 cm), 7% leaves, 2% soil. |
| Diehl (1997) | Multiple | 144 field investigations of driftwood accumulations at bridges across the USA | Predominantly natural wood: two small accumulations contained 50% trash, three accumulations largely saw logs from storage areas, one contained parts of a boat and dock, for the other accumulations the presence of human artefacts was insignificant. |
| Bayón et al. (2023, 2023b) | 63 flood events in 46 countries | Urban, worldwide | Of 269 photos with debris ('urban flood drifters') present in streets or rivers, 37% of the photos contained vehicles (predominantly cars), 7% furniture, 22% plastic debris, 21% construction debris, 18% woody debris, 10% metal debris and 9 % other debris. |

109 Therefore, *this study aims* to characterise bridge clogging in Belgium and Germany during the 2021
 110 floods and to determine the effect of bridge design, bridge location and hydraulic conditions on the
 111 observed clogging.

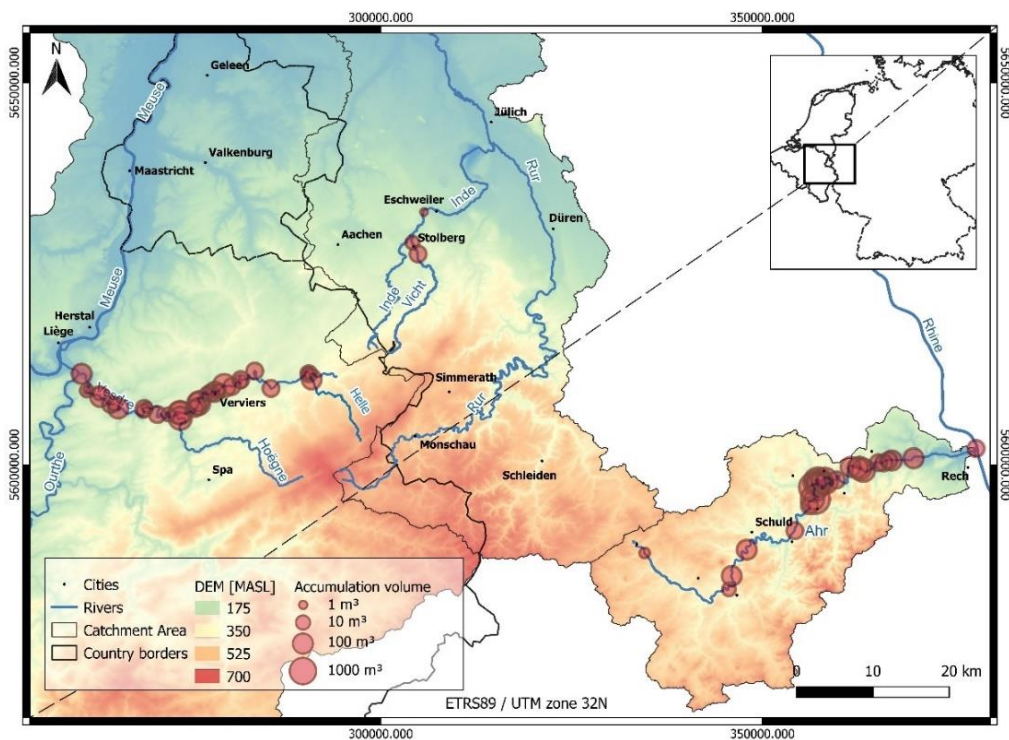
112 2. Methodology

113 2.1. Study area

114 For this study, the clogging of bridges along six rivers in Belgium and Germany during the 2021 flood
 115 event was investigated. The rivers Ahr, Inde and Vicht are situated (largely) in western Germany, the
 116 Vesdre, Helle and Hoëgne (largely) in Belgium (Figure 2, Table 2). The Ahr, which originates in
 117 Blankenheim at 520 m above sea level and joins the river Rhine near Sinzig, is the largest river in this
 118 study (Table 2) and the only one that belongs to the Rhine catchment area. It is characterised by steep
 119 hillsides and confined bedrock of sandstone, siltstone and clay slate. The share of urban areas
 120 increases in downstream direction, while the catchment area is dominated by forests and grasslands
 121 towards the source (MKUEM, 2019). The other five studied rivers are all part of the Meuse catchment.

122 The *Vicht* is a tributary of the *Inde*, which eventually joins the Rur in Germany. The Inde's discharge is
123 regulated by a drinking water reservoir, the Wehebachtalsperre, at the Wehebach tributary.

124 In Belgium, debris accumulation was studied at the river Vesdre, and its tributaries Helle and Höegne.
125 The *Vesdre* (Weser in German) originates in the High Fens plateau in north-eastern Wallonia. After
126 70 km, near Liège, it joins the Ourthe, i.e. the main Belgian tributary of the Meuse. The Vesdre dam
127 (also called Eupen dam) just before the town of Eupen and the La Gileppe dam regulate discharge in
128 the upper part of the catchment, and provide drinking water reservoirs of approximately 25 Mm³
129 each. The lower part of the Vesdre region is mostly characterised by urban and industrial areas
130 (Bauwens et al., 2011). The *Helle* (Hill in German) also originates in the High Fens plateau and merges
131 with the Vesdre in Eupen (Vesdre river km 55, measured from its mouth). Upstream of the city of
132 Eupen, a part of the Helle discharge is diverted through a tunnel into the aforementioned Vesdre dam
133 (Bruwier et al., 2015). Lastly, the *Hoëgne* joins the Vesdre at Pepinster. The Hoëgne is not regulated
134 by reservoirs, causing periodic flood events (Bruwier et al., 2015). Both the Helle and Hoëgne have
135 comparatively steep slopes, of 1.6% and 1.7% (Table 2).



136
137 Figure 2: Map of the study area and the studied rivers, with debris accumulations indicated.

138

139 *Table 2: Characteristics of the rivers examined in this study, including physical characteristics, average annual discharge and*
 140 *estimated peak discharge during the 2021 flood. Sources: (Bauwens et al., 2011; Bruwier et al., 2015; Cuvelier et al., 2018;*
 141 *Deroanne & Petit, 1999; Eifel-Rur, 2021a, 2021b; LfU, 2023; MKUEM, 2019; NRW, 2023a, 2023b)*

| | Tributary of | Catchment area [km ²] | Length [km] | Average slope [%] | Average discharge [m ³ /s] | (Estimated) Discharge during 2021 flood [m ³ /s] |
|--------|-----------------|--------------------------------------|----------------|----------------------|---|---|
| Ahr | Rhine | 900 | 86 | 0.5 | 7 | 800-1200 |
| Inde | Rur | 344 | 47 | 0.7 | 2.8 | >100 |
| Vicht | Inde | 104 | 23 | 1.1 | 0.6 | >100 |
| Vesdre | Ourthe | 683 | 70 | 0.8 | 11 | 660 |
| Helle | Vesdre | 37 | 25 | 1.6 | 1.1 | 340 |
| Hoëgne | Vesdre | 200 | 30 | 1.7 | 3.5 | 265 |

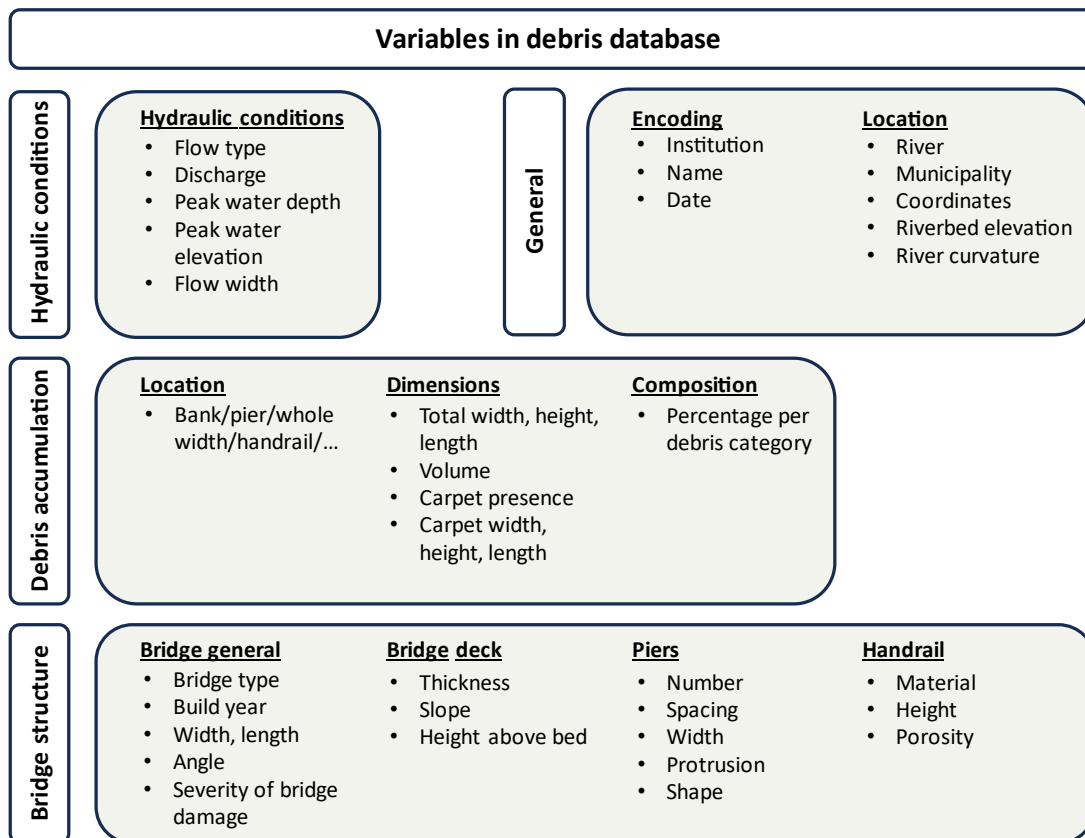
142

143 2.2. Database construction and analysis

144 This paper presents an analysis derived from a database on debris accumulation at bridges in Belgium
 145 and Germany during the 2021 floods (Epicum et al. 2024). A total of 71 bridges affected by debris
 146 clogging were studied (38 in Belgium and 33 in Germany, mainly at the rivers Vesdre resp. Ahr), mostly
 147 based on aerial and handheld photos of the accumulations taken during or just after the flood. This
 148 photo analysis was needed to provide reliable information on the nature of the accumulations, since
 149 field surveys arrived late to investigate debris, when accumulations had often already been removed
 150 and dismantled. The database and analysis focus on three main aspects of debris accumulation, as
 151 summarised in Figure 3:

- 152 (1) **Bridge properties:** bridge location, damage and geometry, including the general bridge design
 153 and properties of the piers, deck and railing.
- 154 (2) Local **hydraulic conditions**, including estimated peak water levels, discharge and the flow
 155 width during the 2021 flood.
- 156 (3) **Accumulation properties**, including estimated accumulation dimensions, its location at the
 157 bridge, and the debris composition.

158 For each of these categories, the main data collection methods for the database and the analysis steps
 159 are discussed below. Further details of the database construction as well as the database itself can be
 160 found in the companion data descriptor (Epicum et al., 2024b).



161
162 *Figure 3: Overview of the main variables documented in the debris database*

163 **2.2.1. Bridge properties**

164 For the bridge properties, the database documents the bridge location, observed damage and the
165 design of the bridge in general, bridge deck, piers and handrail (Figure 3). Bridge properties are based
166 on the following sources:

- 167 (1) Construction drawings, received from the Landesbetrieb Mobilität Rheinland-Pfalz or
168 Deutsche Bahn in Germany, and Service Public de Wallonie in Belgium.
- 169 (2) An online cartographic portal of the 2021 flood event with georeferenced maps and aerial
170 photos for Germany (<https://arcgis.bbk.itzbund.de/arcgis/apps/sites/#/hochwasser2021>)
171 and pre-event georeferenced maps and aerial views for Belgium
172 (www.geoportail.wallonie.be/walonmap).
- 173 (3) In situ measurements (if access to the structure or part of it was possible).
- 174 (4) Post-event pictures.

175 When multiple information sources were available, the first available source on the list was used,
176 ensuring maximum data accuracy with a reasonable measurement effort.

177 **2.2.2. Local hydraulic conditions**

178 Local hydraulic conditions in the database include estimates per bridge of the peak water level,
179 discharge and, for the Ahr valley, the flow width (maximum horizontal extent of the flooded area at
180 the bridge location). Peak water levels and discharges at the Arh are based on reconstructed gauge
181 data from the State Office Landesamt für Umwelt Rheinland-Pfalz in Germany; the flow widths are

182 based on field surveying and estimated coverage of the inundation areas conducted by the same state
183 office (personal communication, 2022). Data for the Inde and Vicht is provided by the WVER
184 Wasserverband Eifel-Rur (personal communication, 2022). In Belgium, water levels are based on a
185 post-event field survey performed by the Walloon Administration. Discharges are based on
186 hydrological modelling of the flood event from distributed rain data performed by Dessers et al.
187 (2023).

188 2.2.3. Accumulation properties

189 Accumulation properties are based on the analysis of handheld and aerial photos taken during or
190 directly after the flood. For the 71 bridges investigated, a total 205 photos with visible debris were
191 used, sourced from local governments, news agencies, inhabitants of the area and social media. The
192 accumulation properties include:

- 193 - The total length, width and height of the accumulation, measured from accumulation edge to
194 edge (e.g. from the most upstream to the most downstream point, measured parallel to the
195 river axis).
- 196 - The accumulation volume, measured by compartmentalizing accumulations into sections
197 (blocks) and estimating the visible width W , length L , height H and hence volume V of each
198 section (for an example, see Figure 3 in Erpicum et al. (2024b)). These volumes are based on
199 the contours of accumulations, so they describe the bulk accumulation volume (including
200 pores), not the solid volume.
- 201 - The debris composition, i.e. the estimated volume fraction of the debris categories listed in
202 Table 3.

203 The software ImageJ (version 1.53) was used to measure lengths and surfaces from pictures, using
204 data from the bridge's geometry or surrounding structures for scale. Information from photos from
205 different perspectives, including aerial and handheld photos, was combined to obtain both horizontal
206 and vertical dimensions. To maximise the accuracy of the estimations, three cases were initially
207 analysed by three different researchers. This resulted in a refined procedure and more stringent
208 definition of parameters, after which remaining variations between researchers were limited, e.g. up
209 to 15% for accumulation volumes. For all following bridges, each evaluation was performed
210 independently by two different researchers. If both estimations differed less than 15%, the average
211 value was encoded in the database. If they differed by 15% or more, results were discussed to get a
212 value approved by both researchers.

213 Based on the debris categories in the database (type A to H in Table 3), debris composition was
214 additionally analysed in terms of debris shape, based on the premise that object shape likely governs
215 the blocking probability, the degree of interlocking between debris pieces and the permeability of
216 both individual debris and the full accumulation. Hereto, the debris volume is categorised as elongated

217 shapes (referred to as ‘logs’), flat shapes (‘plates’) and bulky objects (‘cubes’), in line with previous
 218 studies in coastal engineering, including Wüthrich et al. (2020) and Stolle et al. (2018). The volume of
 219 debris in each of the debris categories is assigned to these three shape classes, following the ratios in
 220 Table 3. This results in an estimate of the fraction of log-shaped, plate-shaped and cuboid debris in
 221 every accumulation, pivotal for the realistic reproduction of accumulations in physical models.

222 *Table 3: The debris categories distinguished in the database, and the ratios used to translate this into volumes of log-shaped,*
 223 *plate-shaped and cuboid debris.*

| Debris type | Log fraction | Plate fraction | Cube Fraction |
|---|--------------|----------------|---------------|
| A - Natural wood (trees) | 1 | - | - |
| B - Anthropogenic wood (construction wood and woody debris) | 0.5 | 0.5 | - |
| C - Plastic tanks and containers | - | - | 1 |
| D - Metal tanks and containers | - | - | 1 |
| E - Vehicles (cars and caravans) | - | - | 1 |
| F - Household items (furniture, appliances) | 0.2 | 0.4 | 0.4 |
| G - Industry items (large installations) | 0.2 | 0.4 | 0.4 |
| H - Building rubble (not fully wooden. E.g. roof parts, insulation) | 0.5 | 0.5 | - |

224 This characterization of the debris accumulations relies on the analysis of photos, and hence on
 225 information visible on photos which were mostly taken after the flood event. This inherently means
 226 that the hidden part of any accumulation is assumed to be of similar composition as the visible outside
 227 surface. Also, the submerged part of accumulations is not visible, leading to an underestimation of
 228 debris volumes, especially for photos taken during the actual flood. Given the difficulty of detailed
 229 field observations in an area where immediate disaster relief and cleaning operations obviously take
 230 precedence, these limitations are deemed acceptable, especially because they allow for systematic
 231 characterization and analysis of bridge clogging in a larger area, rather than at a single bridge.
 232 Nonetheless, these caveats imply that data is more suitable for the overall characterization of bridge
 233 clogging and general trends, than for detailed quantitative conclusions on individual accumulations.

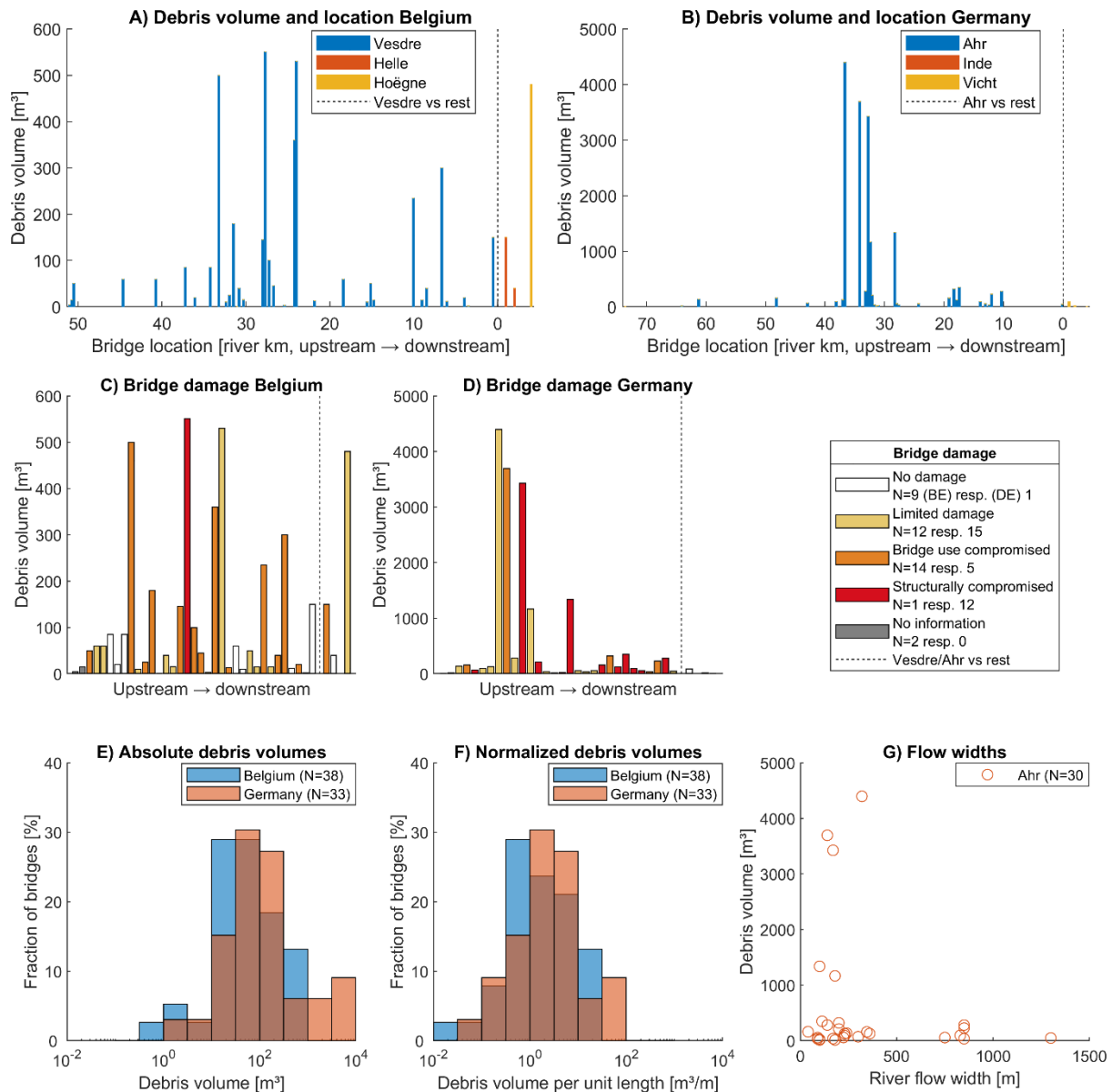
234

235 3. Results

236 3.1. Characterization of clogging

237 To characterise the clogging, it is important to examine the clogging locations, severity and differences
238 between Belgium and Germany. The locations of the clogged bridges are indicated in Figure 2 and
239 Figure 4A, B. In Belgium, 35 of the 38 bridges with clogging in the database are at the Vesdre, two at
240 the Helle and one at the Hoëgne (tributaries of the Vesdre). Clogging was especially severe in Pepinster
241 and Verviers (river km 33 to 24). In Germany, 30 of the 33 clogged bridges in the database are at the
242 Ahr, one at the Inde and two at the Vicht. Clogging was especially severe around Altenahr, Kreuzberg
243 and Pützfeld (river km 37 to 28), with the only observed accumulations of a volume of more than
244 3,000 m³ occurring within this area. Overall, these numbers mean that any comparison of database
245 results between Belgium and Germany for the 2021 flood is very much dominated by the rivers Vesdre
246 resp. Ahr. In both countries, bridge damage was substantial, with overall 18% of the considered
247 bridges structurally compromised and a further 27% too damaged to be used (Figure 4C, 4D). On
248 average, damage was more severe at the bridges with larger accumulations.

249 Comparing the accumulations in both countries, accumulations in Germany were generally larger,
250 with a mean debris volume of 118 m³ in Belgium vs 518 m³ in Germany. Part of this is related to the
251 Ahr being wider than the Vesdre. Consequently, normalised volumes of debris per meter of bridge
252 length (i.e. m³/m) decreases the disparity between countries somewhat (Figure 4E, 4F), but
253 normalised debris volumes in Germany still remain larger. Both countries show many relatively small
254 accumulations and a few very large accumulations, overall resulting in a spread of more than three
255 orders of magnitude in the observed debris volumes.



256
 257 *Figure 4: A) Plot of the debris volumes and the location of the blocked bridges in Belgium, measured along the path of the*
 258 *river Vesdre. Negative values indicate bridges on the Helle and Hoëgne (tributaries). B) Idem for Germany, with river km*
 259 *measured along the Ahr, negative values for the Inde and Vicht (different catchments). Note the different y-axis. C) and D)*
 260 *Bridge damage in both countries, plotted in the same order as subplot A and B, but evenly spread over the x-axis. Note the*
 261 *different y-axes. E) Comparison of absolute debris volumes at Belgian and German bridges. NB: logarithmic x-axis. F) Idem,*
 262 *with volumes normalised by bridge length. G) The width of the flooded area (river width) vs debris volumes for the river Ahr.*

263 The actual flow width (width of the inundated area) during the flood was generally much wider than
 264 the river channel or bridge under “normal” conditions. The analysed data only contains flow widths
 265 for the Ahr bridges, showing a mean flow width of 330 m, compared to a mean bridge length of 55 m.
 266 This implies that substantial overbank flow and flooding occurred. Notably, the large accumulations
 267 occurred at relatively narrow flow widths (Figure 4G). Likely, this is explained by locations with the
 268 widest flow having had large flooded areas where debris could deposit, aided by trees, buildings and
 269 other obstacles in the floodplains that were able to catch floating debris. Contrarily, at places with a
 270 more constricted river, debris likely tended to follow the river channel, thus decreasing the chances
 271 of being stuck along the way and increasing those of reaching the bridge.

272 3.2. Case studies: extreme accumulations

273 A closer examination of the largest accumulations, presented in Table 4, shows substantial variation
274 between cases. The largest accumulation, approximately 4,400 m³ consisting primarily of trees,
275 occurred at the riverbank right next to a bridge in Pützfeld, Germany (Figure 5A). The debris' location
276 against the railway track (built as a raised embankment) means the debris accumulation likely
277 generated relatively limited flow resistance and backwater rise. However, it shows the large amount
278 of debris transported during the flood, which could under different circumstances (e.g. different river
279 curvature or bridge angle) accumulate in the river channel. The second largest accumulation (Figure
280 5B, ~3,700 m³) is completely different, with a very dense accumulation in the channel in front of a
281 railway bridge. This debris was mainly of anthropogenic (i.e. man-made) origin, including caravans,
282 building rubble and tanks from heating systems. A similar accumulation (slightly less dense, with
283 several cars and slightly more trees) occurred at two parallel bridges in Altenahr, visible on Figure 5C.
284 Accumulations in Belgium were slightly smaller and generally without vehicles, but otherwise
285 comparable in composition. For instance, the two accumulations visible in Figure 5D (in Pepinster,
286 Belgium) both contained a mixture of trees and building rubble. This photo taken during the flood also
287 shows the extent of the flooding and, from the water flowing down into the river in the middle of the
288 photo, the backwater rise caused by the debris accumulation. In addition, the background shows a
289 second clogged bridge, shortly after the first one.



290
291 *Figure 5 Examples of clogged bridges in the database. A) Pützfeld, Germany (bridge id 63 in the database, taken after the*
292 *flood). Photo based on an aerial survey by GeoFly GmbH and provided by Virtual City Systems. B) Kreuzberg, Germany (bridge*
293 *id 62, after the flood). Source: Baumert (2024). C) Altenahr, Germany (bridge id 55 and 56, after the flood). Photo by Polizei*
294 *Thüringen (2021). D) Pepinster, Belgium (foreground: bridge id 59; background: bridge id 60. During the flood) Credit: Vedia.*
295 *The flow direction is from left to right and foreground to background.*

296 *Table 4: A characterization of the five largest accumulations of both countries in the database. Bridge id refers to the id's*
 297 *used in the database by Erpicum et al. (2024). River km gives the distance from the mouth of the respective river. Estimated*
 298 *debris volumes are given in m³ (V) and in m³ per meter of bridge length (V'). Deck height above bed refers to the underside of*
 299 *the deck. For bridges with multiple spans, the minimum span width (minimum distance between piers, or between pier and*
 300 *abutment) is given.*

| Country | Bridge ID | River | Municipality | River km | V [m ³] | V' [m ³ /m] | Water depth [m] | Deck height above bed [m] | Deck thickness [m] | Number of piers | Span width [m] |
|---------|-----------|--------|--------------|----------|---------------------|------------------------|-----------------|---------------------------|--------------------|-----------------|----------------|
| Belgium | 53 | Vesdre | Verviers | 27.7 | 550 | 14 | 7.2 | 6.0 | 1.0 | 3 | 6.4 |
| | 60 | Vesdre | Pepinster | 24.1 | 530 | 19 | 7.6 | 3.7 | 1.5 | 2 | 8.2 |
| | 112 | Hoëgne | Pepinster | 1.2* | 460 | 21 | 4.6 | 3.4 | 1.4 | 1 | 9.3 |
| | 36 | Vesdre | Verviers | 33.2 | 400 | 12 | 7.1 | 4.2 | 1.5 | 2 | 10.5 |
| | 59 | Vesdre | Pepinster | 24.2 | 360 | 13 | 6.3 | 3.1 | 1.0 | 2 | 7.8 |
| Germany | 63† | Ahr | Pützfeld | 36.7 | 4396 | 88 | 4.0 | 3.3 | 1.0 | 3 | 10.0 |
| | 62 | Ahr | Kreuzberg | 34.2 | 3695 | 62 | 9.0 | 4.5 | 0.8 | 3 | 5.5 |
| | 56‡ | Ahr | Altenahr | 32.4 | 3424 | 53 | 6.8 | 4.9 | 1.5 | 2 | 9.0 |
| | 47 | Ahr | Altenahr | 32.4 | 1337 | 27 | 9.0 | 5.8 | 1.3 | 1 | 20.0 |
| | 55‡ | Ahr | Altenahr | 28.1 | 1165 | 19 | 6.8 | 5.0 | 1.2 | 4 | 10.0 |

301 *1.2 km from the confluence with the Vesdre, which is at Vesdre river km 24.0.

302 †Debris accumulation located at the riverbank directly next to bridge.

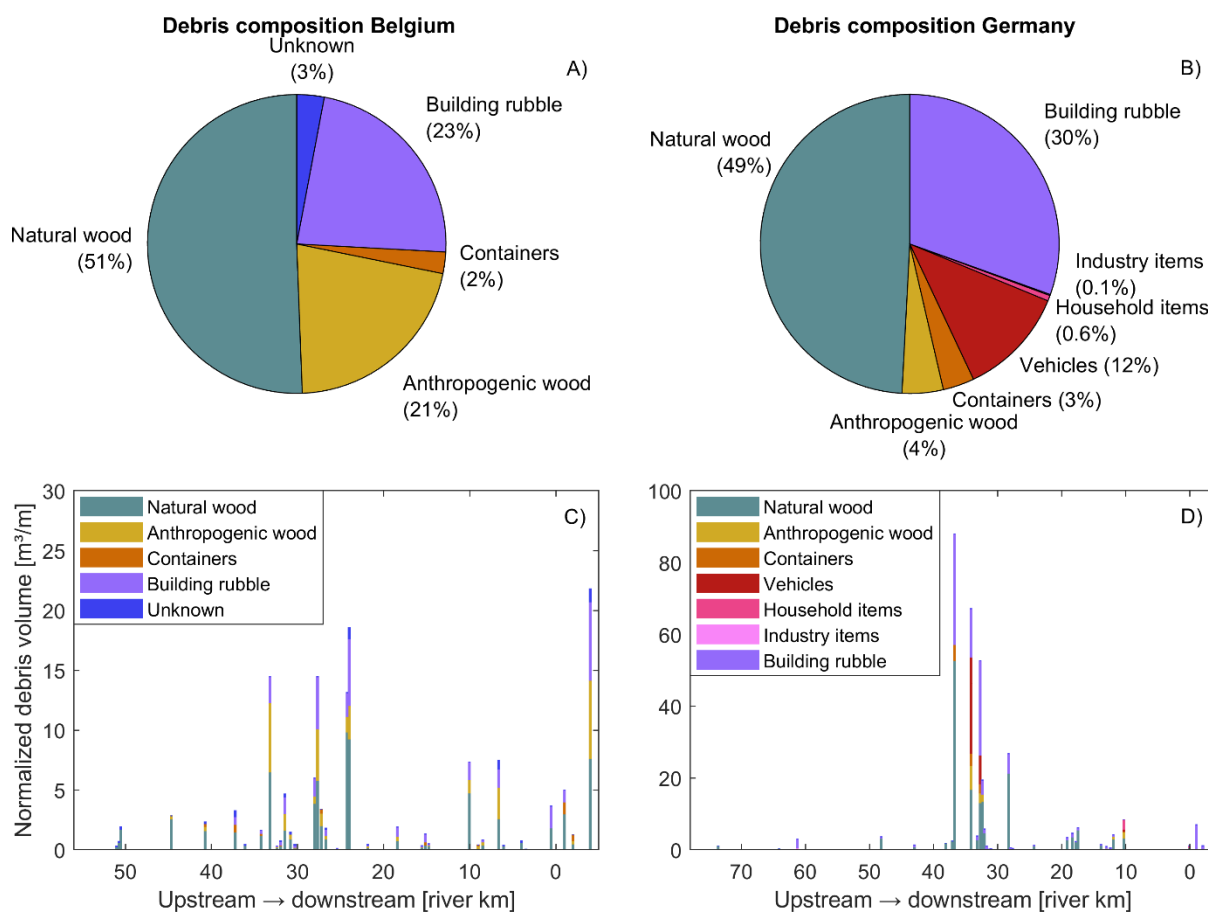
303 ‡Bridge 55 and 56 form a twin bridge, i.e. a road and railroad bridge about 15 m apart.

304 3.3. Debris contents

305 A multitude of different objects and materials was present in the debris accumulations, as visible in
 306 photos of accumulations (e.g. Figure 1, Figure 5). Detailed analysis of the type and volume of objects
 307 in the accumulations showed that on average about half of the material was natural wood (trees), in
 308 both Belgium and Germany (Figure 6A, 6B). The other half of the debris mixture was of anthropogenic
 309 origin, often in the form of anthropogenic wood (construction wood, cut and without bark) or building
 310 rubble (parts of roofs, insulation material, etc.) from upstream buildings destroyed by the flood. In
 311 Germany, a substantial fraction of the debris also consisted of vehicles: cars and caravans. These were
 312 not present on the photos of Belgian accumulations, probably because campsites or parking areas
 313 were not located directly along the river or not flooded as severely. Other debris types present are
 314 tanks and containers (shipping containers, water tanks, petroleum tanks of heating systems, etc),
 315 household items (furniture, electrical appliances) and industrial items (large equipment from factories
 316 along the river).

317 The composition of individual accumulations is shown in Figure 6C and 6D for all clogging events
 318 investigated in the present study (Figure 2). Overall, data showed different compositions at various
 319 bridges, showing a clear dependence on the geographical location as well as on the land use of the
 320 riverbanks. As an example, data shows that the overall vehicle volume in Germany is largely caused
 321 by the accumulation at river kilometre 34 that contained a large number of caravans (see the photo
 322 in Figure 5B). It shows the dependence of the debris composition on the local presence of
 323 transportable objects or materials, such as caravans at a campsite along the river. Similarly, the large
 324 accumulation volumes and high building rubble content around Ahr river kilometre 35 – i.e. the heavily

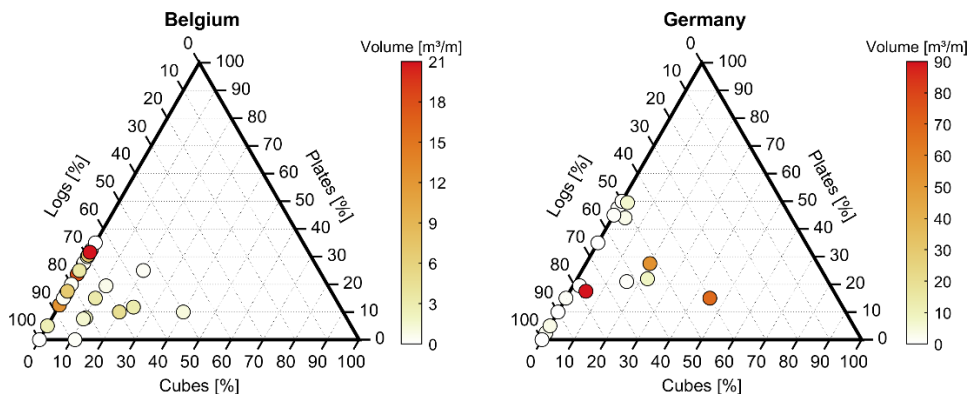
325 damaged towns of Altenahr and Kreuzberg – show that the debris volume and composition at bridges
 326 are directly linked to the local flooding severity and damage in an area.



327
 328 *Figure 6: The composition of the accumulations in Belgium (subplot A and C) and Germany (B and D). The top row shows the*
 329 *volume fractions of the total debris volume per country, the bottom row the composition per accumulation.*

330 The shape of the objects in the accumulations was analysed by examining the debris categories
 331 (Figure 6). Visual observations showed the presence of three main features: (1) elongated one-
 332 dimensional objects (here called ‘logs’); (2) flat two-dimensional objects (‘plates’) and (3) voluminous
 333 three-dimensional objects (‘cubes’ or ‘cuboids’) in each of the categories, as previously discussed in
 334 Table 3. Due to the large fraction of natural wood present, all accumulations predominantly consisted
 335 of 1D log-shaped objects, as shown in Figure 7, where the percentage of all shapes is visualised in a
 336 triangular distribution. Accumulations consisting almost entirely of trees are plotted in the lower left
 337 corner of the triangles, including the largest accumulation of Germany (also shown in Figure 5A).
 338 Accumulations with logs and plates are plotted along the left edge of the triangle, including the largest
 339 accumulation of Belgium. Plate material reaches up to 35% in Belgium, 50% in Germany, often
 340 stemming from a high fraction of building rubble – where roof parts or insulation material are
 341 examples of flat objects – sometimes also from anthropogenic wood and household items. The
 342 accumulations belonging to the rightmost circles in both triangles are characterised by their high cube
 343 content (up to 45%), from tanks and containers in Belgium, mostly from vehicles in Germany. Lastly,
 344 there are a few accumulations with a substantial content of all three debris shapes, in the middle of

345 the triangles: e.g. three in Germany with 15%-25% cuboid objects, 20%-30% plate and 50%-65% logs.
 346 Overall, the large accumulations – which are most interesting from a water safety perspective – show
 347 especially in Germany quite mixed debris shapes.



348
 349 *Figure 7: The estimated fraction of log-, plate- and cube-shaped objects in the debris accumulations. Each circle represents*
 350 *an accumulation in the database, colour-coded by volume, with its location along the three axes indicating the volume*
 351 *fraction of log-, plate- and cube-shaped objects in the debris mixture.*

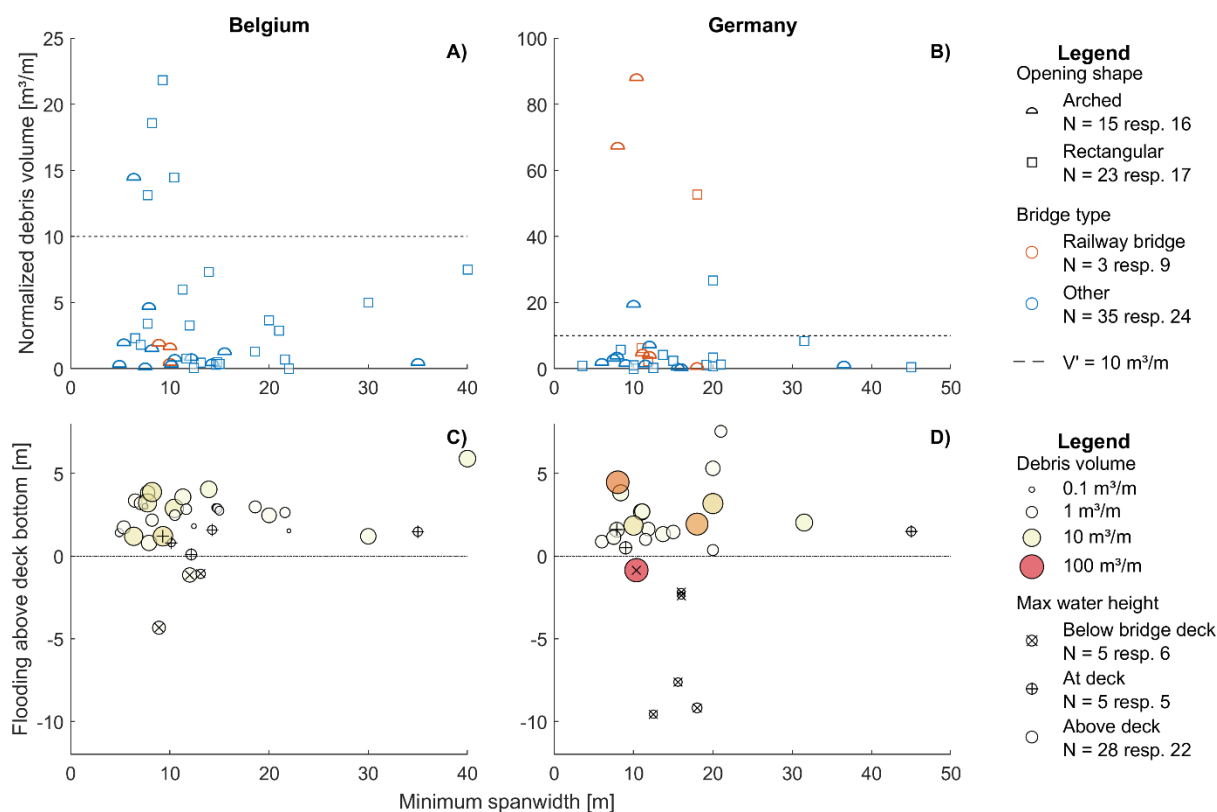
352 3.4. Effects of bridge design and hydraulic conditions

353 Accumulation volumes were linked to bridge designs and hydraulic conditions. Bridges can block
 354 debris and affect debris accumulation at their piers and deck. While the piers can block passing debris
 355 during regular conditions, effects from the deck and railing are only possible if the water level reaches
 356 the deck (or if the emerged part of floating debris is sufficiently high to collide with the deck). During
 357 the flood, most bridges in the database had (peak) water levels above the top of the bridge deck
 358 (Figure 8), meaning both the piers and deck generally contributed to a debris blocking.

359 Span width, i.e. the horizontal distance between piers or abutments, is known from literature to be a
 360 major influence on the *probability* of debris blockage (Diehl, 1997). A similar effect on accumulation
 361 *volume* is visible in our database (Figure 8). Most large accumulations occurred at span widths of
 362 approximately 10 metres or less, where trees longer than the distance between piers initiated
 363 clogging. Nonetheless, clogging also occurred at bridges without piers, where the abutments were too
 364 far apart to be bridged by trees (e.g. the upper right point in Figure 8C, with a span width of 40 m).
 365 The shape of bridge openings had little effect (Figure 8A, 8B) as data shows little difference between
 366 bridges with arched or rectangular openings. However, it is noticeable that the three largest
 367 accumulations in Germany were all railway bridges. Lastly, one can note that accumulations with more
 368 than 10 m³/m are relatively rare in both countries; they make up 14% of the number of clogged
 369 bridges.

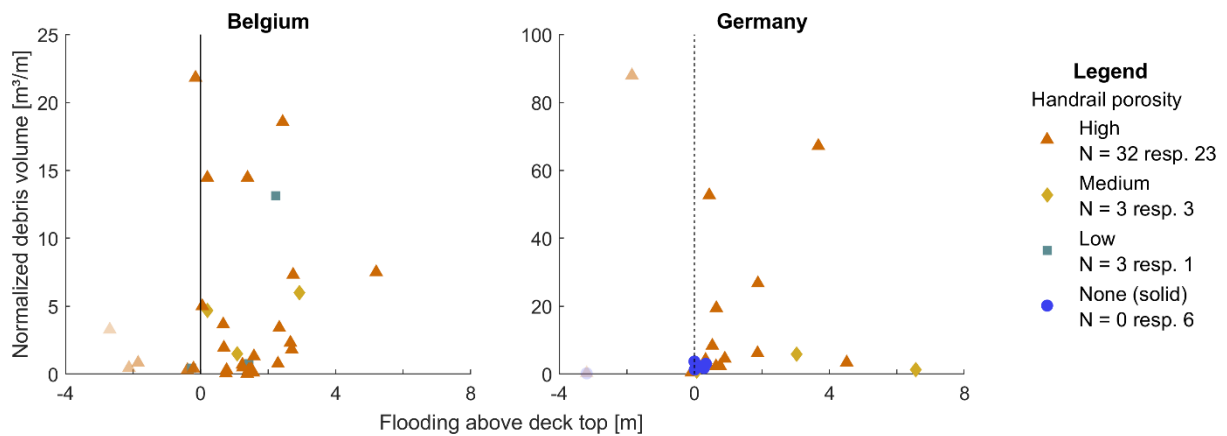
370 A limited freeboard (the distance between deck and water level) is also known to increase the
 371 *probability* of blocking (Schmocker & Hager, 2011). For the 2021 flood event, flooding was so extreme
 372 that peak water levels reached or exceeded the bridge deck for 85% of the studied bridges (circles
 373 above the dashed line in Figure 8C, 8D), frequently exceeding it by several meters. Almost all

374 substantial accumulations occurred when the water level reached or exceeded the bridge deck,
 375 supporting the importance of the bridge deck and railing for the occurrence of large accumulations.



376
 377 *Figure 8: The effect of span width and (subplot A, B) bridge design or (C, D) maximum water levels on accumulation volumes*
 378 *in (A, C) Belgium and (B, D) Germany. Note: maximum water levels are indicated relative to the bottom of the bridge deck.*
 379 *Straight crosses in symbols indicate a flood height between the bottom and top of the deck. Generally, the largest debris*
 380 *volumes occurred at bridges where the span width was limited ($\leq 10 \text{ m}$) and the water level reached or exceeded the deck.*

381 Regarding railings, most bridges in the database have permeable metal structures, but in some cases
 382 solid stone walls are used. Figure 9 shows handrail porosities, debris volumes and water heights
 383 relative to the edge between the bridge deck and railing. For both countries, the largest accumulations
 384 occurred for highly permeable handrails, suggesting that the flow through the handrail might play a
 385 role in the accumulation process. In Belgium, no impermeable walls were present in the database, but
 386 in Germany, these impermeable railings (stone walls, indicated by blue circles) had considerably lower
 387 debris volumes. Interlocking of debris with permeable handrails likely played a role here in maintaining
 388 accumulations and preventing debris flowing over the bridge. Conversely, impervious handrails cause
 389 more flow resistance and backwater rise, leading to earlier overflow, and possibly earlier release of
 390 debris. Also, handrail damage may have enabled easier transport of debris over the bridge. However,
 391 firm statistically significant conclusions are difficult to draw since only at three impermeable railings
 392 water is actually estimated to have reached the railing. For the other impermeable railings, interaction
 393 between handrail and debris would only be possible for large objects floating on the water or for
 394 inaccurate height estimations. This means that the sample size in the current database is rather limited
 395 and further examination of the effect of low, medium and high handrail porosities (squares, diamonds
 396 and triangles in Figure 9) on accumulated debris volumes shows no clear trend.



397
398
399
400
401
402

Figure 9: The effect of handrail porosity and flooding height on debris volumes in Belgium and Germany. The vertical dashed line indicates where peak water levels reached the edge between deck and handrail. Markers with lower water levels than this have increasing transparency to indicate the decreasing likelihood of debris interacting with the handrail. High porosity refers to handrail with thin elements and large spacing, medium to thin elements with low spacing, low to broad elements with low spacing and no porosity to solid walls.

403 4. Discussion

404 4.1. Debris content

405 Highly heterogeneous debris contents appeared as one of the typical features of the July 2021 flood
406 in Belgium and Germany, with approximately half of the total debris volume of man-made origin,
407 containing large amounts of building rubble (parts of roofs, walls, insulation, etc) and construction
408 wood, smaller amounts of tanks, containers and household items (furniture, appliances) and
409 occasionally vehicles (cars, caravans) in addition to trees. Typically, previous investigations reported
410 accumulations that consisted almost entirely of trees, also referred to as ‘log jam’ or ‘large wood
411 accumulation’. As an example, in field investigations of 144 floating debris accumulations at bridges
412 throughout the United States (Diehl, 1997), two small accumulations appeared to have a 50/50 split
413 between trash and woody debris, one contained parts of a boat and dock; in all others the role of
414 man-made objects was insignificant. This is the consequence of floods mostly occurring in natural
415 areas, where bank erosion and flooding of forests along the river can bring large amounts of trees into
416 the river (Diehl, 1997; Lucía et al., 2015; Rickenmann, 1997; Steeb et al., 2017). Nonetheless, large
417 amounts of man-made objects have been reported before at floods in more urbanised areas. For
418 instance, in a photo analysis of debris in rivers and streets after 63 floods in urbanised areas (Bayón
419 et al., 2023, 2024), woody debris, plastic and building rubble were each visible on approximately 50%-
420 60% of the *photos*, and affected vehicles on 35% of the photos. This is likely due to their focus on
421 urbanised areas compared to the mix of urban and natural areas hit by the 2021 flood. Indeed, in our
422 analysis, trees were visible on the large majority of photos, and made up approximately 50% of the
423 *debris volume*. Similar observations were made during coastal flooding, where tsunamis and storm
424 surges transported a large number of heterogeneous debris that accumulated as coastal structures,
425 forming heavily packed ‘*debris-dams*’ (Chock et al., 2013).

426 For natural woody debris, previous experiments repeatedly showed the importance of debris size,
427 shape and type. Logs are less easily transported when they are longer, thicker or have rootstock

428 (Braudrick & Grant, 2000; Diehl, 1997). Once in transport, the probability of wood pieces to be blocked
429 at bridges increases with increasing log length (Bezzola et al., 2002; Diehl, 1997; Gschnitzer et al.,
430 2017; Schalko et al., 2020; Schmocker & Hager, 2011); with increasing stiffness (Hartlieb, 2015); or
431 with increasing branching or rootstock presence (Bezzola et al., 2002; Gschnitzer et al., 2017). Once
432 blocked, backwater rise increases with increasing specific density (Hartlieb, 2015) and decreasing log
433 thickness (Follett et al., 2020; Schalko et al., 2019) – similar to how the flow rate of groundwater is
434 lower in finer soils. Accordingly, mixtures with a higher organic fine material content (leaves, twigs)
435 between logs also create more backwater rise (Schalko, 2018; Schalko et al., 2019). Hence, for debris
436 mixtures with both man-made materials and natural wood, which inherently have an even larger
437 spread in size, shape and density, debris properties must affect the accumulation process and
438 backwater rise even more. Honingh et al. (2020) demonstrated that debris mixtures with plastic bags
439 and bottles create denser accumulations and can more than double the backwater rise compared to
440 pure logjams. Studies on more diverse mixtures or larger objects are scarce, but it stands to reason
441 that observed impermeable flat objects, such as plastic sheet, sheet wood or wall panels from
442 collapsed caravans (Figure 5B, 5C), lead to denser and less permeable accumulations and therefore to
443 more backwater rise. This is supported by pictures of some accumulations (e.g. Figure 5B), which seem
444 to form dams with low porosity and permeability. On the other hand, cuboid objects (containers) have
445 been shown to exhibit a lesser interlocking nature and be washed away more easily by wave events
446 (Wüthrich et al., 2020), so the same likely applies to cuboid objects in river accumulations. Apart from
447 shape effects, man-made objects also exhibit more variation in material and hence density. Denser
448 objects in the mixture, which are more easily pulled down (or even sink instead of floating), facilitate
449 the generation of an accumulation that extends deeper into the water column instead of forming a
450 floating carpet, thereby increasing backwater rise. Overall, these effects point towards mixed debris
451 causing denser accumulations and more backwater rise. However, more research is needed to confirm
452 and especially quantify these effects.

453 4.2. Bridge design

454 Analysis of the bridge designs and accumulations showed that bridges with large accumulations tend
455 to have some common features. First and foremost, almost all large accumulations in both countries
456 occurred at bridges with limited span widths. It was already well-known that the accumulation risk
457 increases greatly at limited span widths, where a single tree can bridge the distance between two
458 piers (or the abutments) and initiate clogging (Bocchiola et al., 2008; Diehl, 1997; Lange & Bezzola,
459 2006; Schmocker & Hager, 2011). However, the exact span widths at risk depend directly on the length
460 of waterborne trees, and thus on the trees found in an upstream area. Hence, this study provides
461 valuable quantification, that in this area a pier spacing of 10 metres or less substantially increases the
462 debris accumulation risk. This is something that should be taken into account in the reconstruction of
463 damaged bridges.

464 Furthermore, at almost all bridges with large accumulations, peak water levels reached or exceeded
465 the deck. A few clogged bridges reported water levels below the deck – five in Belgium and six in
466 Germany. Any causality between water levels and debris accumulation is likely bi-directional, with
467 high water levels at the deck allowing for blockage by the deck and hence larger accumulations, while
468 larger accumulations simultaneously cause more backwater rise. The importance of blockage at the
469 deck and railing is further supported by clear cases of blocking by the deck, such as in Figure 1, where
470 debris interlocks with the bridge deck and arch, at a bridge without piers. Moreover, the severity of
471 the flood, with sometimes the bridge deck being flooded by 5 metres of water, means that debris
472 could also pass *over* bridges (cf. Piton et al., 2020 on debris release at dams). Here, the design of the
473 bridge superstructure plays a role in the degree of interlocking that occurs between debris and bridge.
474 For instance, porous handrails are known to cause more debris to be stuck in the handrail (Schmocker
475 & Hager, 2011), potentially fixing debris in place when water levels rise until (well) above the bridge
476 deck.

477 Although the role of the deck and railing have received some attention in the past (Bezzola et al., 2002;
478 Gschnitzer et al., 2017; Schmocker & Hager, 2011), most research has focused on the interaction
479 between bridge piers and debris (e.g. De Cicco et al., 2020; Lagasse et al., 2010; Lyn et al., 2007; Panici
480 & de Almeida, 2020; Panici & de Almeida, 2018; Schalko et al., 2020). The fact that 85% of the clogged
481 bridges in the database experienced water levels at or above the deck calls for more specific research
482 on the impact of deck and handrail design on bridge clogging. And as a more immediate implication
483 for practice, the widespread bridge flooding and large water depths over the bridge (Figure 8) imply
484 that building higher bridges could have large safety benefits, decreasing flow resistance and backwater
485 rise by the deck itself, debris blockage by the deck, damage to the bridge and the likelihood of the
486 bridge being unusable during or after a flood.

487 Regarding bridge types, the three largest accumulations in Germany were remarkably all railway
488 bridges. It is possible that the raised construction of the connecting railway on embankments blocked
489 debris (e.g. Figure 5A) or funnelled it toward the bridge, whereas roads would normally be constructed
490 at lower elevations and therefore allow for more overland passage of debris. However, this hypothesis
491 cannot be substantiated by data, given the low number of railway bridges within the dataset, as well
492 as the absence of a similar trend in Belgium. Since the number of entries in the database was limited
493 by the availability of bridges with both debris accumulation photos and corresponding structural data,
494 this also calls for future research on bridge clogging during floods.

495 Lastly, we want to stress that debris clogging at bridges not only depends on the bridge design and
496 hydraulic conditions, but also on the debris that reaches that location. This means that for blockage
497 at a given bridge, debris must A) be ‘picked-up’ by the flow at some point upstream, B) not be blocked
498 at any bridge in between, C) not be deposited anywhere else before reaching the bridge and D) not

499 simply flow *around* the bridge. Throughout this paper, all these aspects are present. The role of debris
500 generation is visible in the debris composition, where a few bridges blocked a large number of
501 caravans, made possible by the presence of flooded campsites upstream. Blockage at intermediate
502 bridges is inherently present in the many closely spaced bridges in the area, and exemplified by the
503 two clogged bridges in Figure 5D. The same photo illustrates how flooding well outside the actual river
504 channel would allow debris to easily flow around a bridge. The observed trend that the sections of the
505 Ahr with the largest flooded river width have smaller debris accumulations, is probably due to the
506 same principle, and due to debris being trapped by trees, buildings or other obstacles in the flooded
507 area. Overall, the importance of these codependent and chaotic processes means that any correlation
508 between bridge design and debris clogging can easily be hidden. This also points out the need for
509 further research to forecast the volumes of debris that might become available during future floods.

510 5. Conclusions

511 A database of debris clogging at Belgian and German bridges during the 2021 summer floods was
512 developed. The observed debris accumulations at the bridges ranged in volume from a few m³ to more
513 than 4,000 m³, i.e. up to 88 m³ per meter of bridge length. Especially larger accumulations were able
514 to disrupt the flow of the river and cause substantial backwater rise. During the 2021 floods, this
515 intensified the flood consequences, increasing damage in an area already heavily afflicted by this
516 extreme event. To better understand the potential danger that such accumulations can pose and
517 where they are most likely to occur, the characteristics of the accumulations and related bridge
518 features were studied in more detail.

519 About half of the debris volume was identified as man-made materials – building rubble, construction
520 wood, vehicles, furniture, etc – due to flooding occurring in an area with narrow river valleys and
521 towns built in the river floodplains. While most previous research focused on accumulations purely
522 consisting of trees, this study shows that in 2021 trees only accounted for 50% of the average
523 accumulation. This has major implications for the resulting backwater rise, as building rubble,
524 (crushed) caravans and other man-made objects differ in shape, permeability and density from trees.
525 Heterogeneous mixtures can form accumulations with a lower permeability and porosity than pure
526 logjams, causing markedly more backwater rise. As a result, existing relations to estimate the
527 backwater rise of natural accumulations can lead to a dangerous underestimation of the risks when
528 making flood hazard maps or evacuation decisions in more urban environments. Hence, more
529 research on the effect of debris shape and type on backwater rise is urgently needed.

530 Furthermore, the bridge design and damage status at all debris accumulations were studied. The
531 debris accumulations and severity of the flood itself caused 45% of the clogged bridges to be
532 structurally damaged, or otherwise too damaged to be used afterwards. In both countries, the largest
533 accumulations occurred at bridges where the distance between piers was small (≤ 10 m), allowing logs

534 to bridge the distance between piers, thereby initiating further clogging. Simultaneously, at most of
535 the bridges, peak water levels reached at least the bridge deck, and frequently exceeded it by several
536 meters. This has major implications: first, having water reaching the deck means that the deck itself
537 will be responsible for backwater rise, irrespective of the presence of debris. Secondly, it means that
538 the deck and railing can block debris, in addition to the piers. Thirdly, having water well above the
539 deck means debris might flow over the bridge and continue downstream, depending on the degree of
540 debris interlocking. Consequently, the deck and handrail height and design are decisive factors in
541 debris accumulation and backwater rise, and future studies on debris accumulation should explicitly
542 take their role into account.

543 In summary, drawing on data gathered during the 2021 floods in Belgium and Germany, this research
544 offers valuable insights into characterizing debris accumulations and main bridge features that
545 triggered substantial clogging. It is believed that this information will be helpful in better
546 understanding the processes associated with debris accumulation at bridges, as well as supporting the
547 development of targeted debris management strategies to reduce flood risk during future events.

548 [Acknowledgements](#)

549 This research was carried out within the context of Interreg project EMfloodReselience, project no.
550 228, co-funded by the European Regional Development Fund. The authors thank Florence Dütz, Gianni
551 Massin, Mariana Vélez Pérez, Lino Schröter, and Mariia Gimelbrant for their assistance in the photo
552 analysis.

553 [Data availability](#)

554 The dataset used in this paper is described in the data descriptor by Ercicum et al. (2024b), under DOI
555 [10.1038/s41597-024-03907-8](https://doi.org/10.1038/s41597-024-03907-8) and can be found in (Ercicum et al., 2024a)Ercicum et al. (2024), under
556 DOI [10.5281/zenodo.11551195](https://doi.org/10.5281/zenodo.11551195).

557

558 References

- 559 Bänziger, R. (1990). Schwemmholz im Unwettersommer1987. *Schweizer Ingenieur und Architekt*,
560 108(47), 1354. doi: 10.5169/seals-77563.
- 561 Baumert, J. (2024). Flut im Ahrtal: Klagt Staatsanwaltschaft den ehemaligen Landrat an?
562 *Südwestrundfunk*. [https://www.swr.de/swraktuell/rheinland-pfalz/koblenz/entscheidung-
563 wird-ex-landrat-pfoehler-nach-flutkatastrophe-ahrta-angeklagt-100.html](https://www.swr.de/swraktuell/rheinland-pfalz/koblenz/entscheidung-wird-ex-landrat-pfoehler-nach-flutkatastrophe-ahrta-angeklagt-100.html)
- 564 Bauwens, A., Sohier, C., & Degré, A. (2011). Hydrological response to climate change in the Lesse and
565 the Vesdre catchments: contribution of a physically based model (Wallonia, Belgium). *Hydrol.*
566 *Earth Syst. Sci.*, 15(6), 1745-1756. doi: 10.5194/hess-15-1745-2011.
- 567 Bayón, A., Valero, D., & Franca, M. J. (2023). *Electronic supplementary material of 'Urban Flood Drifters*
568 *(UFDs): identification, classification and characterization*. Retrieved 10-01-2024 from
569 <https://github.com/arnaubayon/UFD>
- 570 Bayón, A., Valero, D., & Franca, M. J. (2024). Urban Flood Drifters (UFDs): identification, classification
571 and characterisation. *Journal of Flood Risk Management*, 17(3), e13002. doi:
572 10.1111/jfr3.13002.
- 573 Bezzola, G. R., Gantenbein, S., Hollenstein, R., & Minor, H. E. (2002). Verklauung von
574 Brückenquerschnitten (Blocking of bridge cross-sections). *Proc. Intl. Symposium 'Methoden*
575 *und Konzepte im Wasserbau'*. VAW-Titteilung 175: 87-97, ETH Zurich (in German).
- 576 Bocchiola, D., Rulli, M. C., & Rosso, R. (2008). A flume experiment on the formation of wood jams in
577 rivers. *Water Resources Research*, 44(2). doi: 10.1029/2006WR005846.
- 578 Braudrick, C. A., & Grant, G. E. (2000). When do logs move in rivers? *Water Resources Research*, 36(2),
579 571-583. doi: 10.1029/1999WR900290.
- 580 Bruwier, M., Epicum, S., Piroton, M., Archambeau, P., & Dewals, B. J. (2015). Assessing the operation
581 rules of a reservoir system based on a detailed modelling chain. *Nat. Hazards Earth Syst. Sci.*,
582 15(3), 365-379. doi: 10.5194/nhess-15-365-2015.
- 583 Burghardt, L., Klopries, E.-M., & Schüttrumpf, H. (2024a). Structural damage, clogging, collapsing:
584 Analysis of the bridge damage at the rivers Ahr, Inde and Vicht caused by the flood of 2021.
585 *Journal of Flood Risk Management*, e13001. doi: 10.1111/jfr3.13001.
- 586 Burghardt, L., Poppema, D. W., Bénet, L., Wüthrich, D., Epicum, S., & Klopries, E.-M. (2024b). Multi-
587 lab investigation of the effect of debris composition on bridge clogging during floods. In R. M.
588 Boes, I. Albayrak, S. Felder, B. Crookston, & V. Heller, 10th International Symposium on
589 Hydraulic Structures (10th ISHS), ETH Zurich, Zurich, Switzerland.
- 590 Chock, G., Robertson, I., Kriebel, D., Francis, M., & Nistor, I. (2013). Tohoku, Japan, earthquake and
591 tsunami of 2011: Performance of structures under tsunami loads.
- 592 Comiti, F., Lucía, A., & Rickenmann, D. (2016). Large wood recruitment and transport during large
593 floods: a review. *Geomorphology*, 269, 23-39.

594 Cuvelier, T., Archambeau, P., Dewals, B., & Louveaux, Q. (2018). Comparison Between Robust and
595 Stochastic Optimisation for Long-term Reservoir Management Under Uncertainty. *Water*
596 *Resources Management*, 32(5), 1599-1614. doi: 10.1007/s11269-017-1893-1.

597 De Cicco, P. N., Paris, E., Ruiz-Villanueva, V., Solari, L., & Stoffel, M. (2018). In-channel wood-related
598 hazards at bridges: A review. *River Research and Applications*, 34(7), 617-628. doi:
599 10.1002/rra.3300.

600 De Cicco, P. N., Paris, E., Solari, L., & Ruiz-Villanueva, V. (2020). Bridge pier shape influence on wood
601 accumulation: Outcomes from flume experiments and numerical modelling. *Journal of Flood*
602 *Risk Management*, 13(2), e12599.

603 Deroanne, C., & Petit, F. (1999). Longitudinal evaluation of the bed load size and of its mobilisation in
604 a gravel bed river. In *Floods and Landslides: Integrated Risk Assessment* (pp. 335-342).
605 Springer.

606 Dessers, C., Archambeau, P., Dewals, B., Epicum, S., & Piroton, M. (2023). Hydrological modelling of
607 July 2021 floods in Vesdre and Amblève catchments. EGU General Assembly, Vienna, Austria.

608 Diehl, T. H. (1997). *Potential drift accumulation at bridges* (Report nr FHWA-RD-97-028). US
609 Department of Transportation: Federal Highway Administration.

610 Eifel-Rur, W. (2021a). *Die Inde*. <https://wver.de/fluss/die-inde/>

611 Eifel-Rur, W. (2021b). *Die Vicht*. <https://wver.de/fluss/die-vicht/>

612 Epicum, S., Poppema, D. W., Burghardt, L., Benet, L., Klopries, E.-M., Wüthrich, D., & Dewals, B.
613 (2024a). *Database - Bridge clogging and debris - July 2021 flood* Version 1.0). doi:
614 10.5281/zenodo.11551195

615 Epicum, S., Poppema, D. W., Burghardt, L., Benet, L., Wüthrich, D., Klopries, E.-M., & Dewals, B.
616 (2024b). A dataset of floating debris accumulation at bridges after July 2021 flood in Germany
617 and Belgium. *Scientific Data*, 11(1), 1092. doi: 10.1038/s41597-024-03907-8.

618 Follett, E., Schalko, I., & Nepf, H. (2020). Momentum and Energy Predict the Backwater Rise Generated
619 by a Large Wood Jam. *Geophysical Research Letters*, 47(17). doi: 10.1029/2020GL089346.

620 Gschnitzer, T., Gems, B., Mazzorana, B., & Aufleger, M. (2017). Towards a robust assessment of bridge
621 clogging processes in flood risk management. *Geomorphology*, 279, 128-140. doi:
622 10.1016/j.geomorph.2016.11.002.

623 Hartlieb, A. (2015). *Schwemholz in Fließgewässern--Gefahren und Lösungsmöglichkeiten*.
624 *Habilitationsschrift*. Technische Universität München.

625 Honingh, D., van Emmerik, T., Uijttewaal, W., Kardhana, H., Hoes, O., & van de Giesen, N. (2020). Urban
626 River Water Level Increase Through Plastic Waste Accumulation at a Rack Structure [Brief
627 Research Report]. *Frontiers in Earth Science*, 8. doi: 10.3389/feart.2020.00028.

628 Jannaschk, J. (2021). *"Haben so etwas wie dieses Hochwasser in der Form und Intensität noch nie*
629 *erlebt": Feuerwehrmann berichtet von der Lage vor Ort im Katastrophengebiet Ahrweiler.*

630 Watson. <https://www.watson.de/leben/nah-dran/611491321-flut-katastrophe->
631 [feuerwehrmann-berichtet-vor-ort-von-der-lage-in-ahrweiler](https://www.watson.de/leben/nah-dran/611491321-flut-katastrophe-feuerwehrmann-berichtet-vor-ort-von-der-lage-in-ahrweiler)

632 Journée, M., Goudenhoofd, E., Vannitsem, S., & Delobbe, L. (2023). Quantitative rainfall analysis of
633 the 2021 mid-July flood event in Belgium. *Hydrol. Earth Syst. Sci.*, 27(17), 3169-3189. doi:
634 10.5194/hess-27-3169-2023.

635 Kimura, N., Tai, A., & Hashimoto, A. (2017). Flood caused by driftwood accumulation at a bridge.
636 *International Journal of Disaster Resilience in the Built Environment*, 8(5), 466-477.

637 Koks, E. E., Van Ginkel, K. C. H., Van Marle, M. J. E., & Lemnitzer, A. (2021). Brief communication:
638 Critical infrastructure impacts of the 2021 mid-July western European flood event. *Natural*
639 *Hazards and Earth System Sciences*, 22(12), 3831-3838. doi: 10.5194/nhess-22-3831-2022.

640 Korswagen, P. A., Harish, S., Oetjen, J., & Wüthrich, D. (2022). *Post-flood field survey of the Ahr Valley*
641 *(Germany): building damages and hydraulic aspects*. D. U. o. Technology. doi:
642 10.4233/uuid:3cafd772-facd-4e3a-8b1a-cee978562ff1.

643 Lagasse, P. F., Clopper, P. E., Zevenbergen, L. W., Spitz, W. J., & Girard, L. G. (2010). *Effects of debris*
644 *on bridge pier scour*, (NCHRP Rep. 653). Transportation Research Board. doi: 10.17226/22955.

645 Lange, D., & Bezzola, G. R. (2006). Schwemmholz: Probleme und Lösungsansätze. *VAW-Mitteilungen*,
646 188.

647 LfU. (2023). *Pegel Altenahr / Ahr (Gauge Altenahr / Ahr)*. Landesamt für Umwelt (LfU) Rheinland-Pfalz
648 - Hochwasservorhersagezentrale (Environmental Agency of Rhineland-Palatinate - Flood
649 Forecasting Center). [https://www.hochwasser.rlp.de/flussgebiet/ahr/bad-](https://www.hochwasser.rlp.de/flussgebiet/ahr/bad-bodendorf#abfluesse)
650 [bodendorf#abfluesse](https://www.hochwasser.rlp.de/flussgebiet/ahr/bad-bodendorf#abfluesse)

651 Lucía, A., Comiti, F., Borga, M., Cavalli, M., & Marchi, L. (2015). Dynamics of large wood during a flash
652 flood in two mountain catchments. *Nat. Hazards Earth Syst. Sci.*, 15(8), 1741-1755. doi:
653 10.5194/nhess-15-1741-2015.

654 Lyn, D. A., Cooper, T. J., Condon, C. A., & Gan, L. (2007). *Factors in debris accumulation at bridge piers*.
655 Purdue University & U.S. Dept. of Transportation.

656 Manners, R. B., Doyle, M., & Small, M. (2007). Structure and hydraulics of natural woody debris jams.
657 *Water Resources Research*, 43(6). doi: 10.1029/2006WR004910.

658 MKUEM. (2019). *Die Ahr*. Ministerium für Klimaschutz, Umwelt, Energie und Mobilität Rheinland-Pfalz
659 (MKUEM). <https://wasser.rlp-umwelt.de/servlet/is/1210/>

660 Mohr, S., Ehret, U., Kunz, M., Ludwig, P., Caldas-Alvarez, A., Daniell, J. E., Ehmele, F., Feldmann, H.,
661 Franca, M. J., Gattke, C., Hundhausen, M., Knippertz, P., Küpfer, K., Mühr, B., Pinto, J. G.,
662 Quinting, J., Schäfer, A. M., Scheibel, M., Seidel, F., & Wisotzky, C. (2023). A multi-disciplinary
663 analysis of the exceptional flood event of July 2021 in central Europe – Part 1: Event
664 description and analysis. *Nat. Hazards Earth Syst. Sci.*, 23(2), 525-551. doi: 10.5194/nhess-23-
665 525-2023.

666 Naito, C., Cercone, C., Riggs, H. R., & Cox, D. (2014). Procedure for Site Assessment of the Potential for
667 Tsunami Debris Impact. *Journal of Waterway, Port, Coastal, and Ocean Engineering*, 140(2),
668 223-232. doi: 10.1061/(ASCE)WW.1943-5460.0000222.

669 NRW, U. (2023a). *Daten Pegel: Eschweiler* Elektronisches Wasserwirtschaftliches Verbundsystem
670 (ELWAS). <https://www.elwasweb.nrw.de/elwas-web/index.xhtml#>

671 NRW, U. (2023b). *Daten Pegel: Mulartshütte* Elektronisches Wasserwirtschaftliches Verbundsystem
672 (ELWAS). <https://www.elwasweb.nrw.de/elwas-web/index.xhtml#>

673 Oudenbroek, K., Naderi, N., Bricker, J. D., Yang, Y., Van der Veen, C., Uijttewaal, W., Moriguchi, S., &
674 Jonkman, S. N. (2018). Hydrodynamic and debris-damming failure of bridge decks and piers in
675 steady flow. *Geosciences*, 8(11), 409.

676 Pagliara, S., & Carnacina, I. (2011). Influence of large woody debris on sediment scour at bridge piers.
677 *International Journal of Sediment Research*, 26(2), 121-136. doi: 10.1016/S1001-
678 6279(11)60081-4.

679 Panici, D., & de Almeida, G. A. (2020). Influence of pier geometry and debris characteristics on wood
680 debris accumulations at bridge piers. *Journal of Hydraulic Engineering*, 146(6), 04020041.

681 Panici, D., & de Almeida, G. A. M. (2018). Formation, Growth, and Failure of Debris Jams at Bridge
682 Piers. *Water Resources Research*, 54(9), 6226-6241. doi: 10.1029/2017WR022177.

683 Parola, A. C., Apelt, C. J., & Jempson, M. A. (2000). *Debris forces on highway bridges*. Transportation
684 Research Board.

685 Piton, G., Horiguchi, T., Marchal, L., & Lambert, S. (2020). Open check dams and large wood: head
686 losses and release conditions. *Natural Hazards and Earth System Sciences*, 20(12), 3293-3314.

687 Polizei Thüringen. (2021). *Flut hinterlässt Bilder der Zerstörung im Landkreis Ahrweiler*. General-
688 Anzeiger. Retrieved 10-01-2024 from https://ga.de/fotos/region/flutkatastrophe-im-kreis-ahrweiler-bilder_bid-61312581#41

689

690 Rickenmann, D. (1997). Schwemmholz und Wasserkraft. *Wasser Energie Luft*, 89(5-6), 115. doi:
691 10.5169/seals-940182.

692 Rickli, C., Badoux, A., Rickenmann, D., Steeb, N., & Waldner, P. (2018). Large wood potential, piece
693 characteristics, and flood effects in Swiss mountain streams. *Physical Geography*, 39(6), 542-
694 564. doi: 0.1080/02723646.2018.1456310.

695 Robertson, I. N., Riggs, H. R., Yim, S. C., & Young, Y. L. (2007). Lessons from Hurricane Katrina Storm
696 Surge on Bridges and Buildings. *Journal of Waterway, Port, Coastal, and Ocean Engineering*,
697 133(6), 463-483. doi: 10.1061/(ASCE)0733-950X(2007)133:6(463).

698 Ruiz-Villanueva, V., Piégay, H., Gurnell, A. M., Marston, R. A., & Stoffel, M. (2016). Recent advances
699 quantifying the large wood dynamics in river basins: New methods and remaining challenges.
700 *Reviews of Geophysics*, 54(3), 611-652.

701 Saatcioglu, M., Ghobarah, A., & Nistor, I. (2005). Effects of the December 26, 2004 Sumatra earthquake
702 and tsunami on physical infrastructure. *ISET Journal of earthquake technology*, 42(4), 79-94.

703 Schalko, I. (2018). *Modeling hazards related to large wood in rivers* [ETH Zurich]. doi: 10.3929/ethz-b-
704 000293084.

705 Schalko, I., Lageder, C., Schmocker, L., Weitbrecht, V., & Boes, R. M. (2019). Laboratory flume
706 experiments on the formation of spanwise large wood accumulations: I. Effect on backwater
707 rise. *Water Resources Research*, 55(6), 4854-4870. doi: 10.1029/2018WR024649.

708 Schalko, I., Schmocker, L., Weitbrecht, V., & Boes, R. M. (2018). Backwater rise due to large wood
709 accumulations. *Journal of Hydraulic Engineering*, 144(9), 04018056. doi:
710 10.1061/(ASCE)HY.1943-7900.0001501.

711 Schalko, I., Schmocker, L., Weitbrecht, V., & Boes, R. M. (2020). Laboratory study on wood
712 accumulation probability at bridge piers. *Journal of Hydraulic Research*, 58(4), 566-581. doi:
713 10.1080/00221686.2019.1625820.

714 Schmocker, L., & Hager, W. H. (2011). Probability of Drift Blockage at Bridge Decks. *Journal of Hydraulic
715 Engineering*, 137(4), 470-479. doi: 10.1061/(ASCE)HY.1943-7900.0000319.

716 Schmocker, L., & Hager, W. H. (2013). Scale Modeling of Wooden Debris Accumulation at a Debris
717 Rack. *Journal of Hydraulic Engineering*, 139(8), 827-836. doi: 10.1061/(ASCE)HY.1943-
718 7900.0000714.

719 Steeb, N., Rickenmann, D., Badoux, A., Rickli, C., & Waldner, P. (2017). Large wood recruitment
720 processes and transported volumes in Swiss mountain streams during the extreme flood of
721 August 2005. *Geomorphology*, 279, 112-127. doi: 10.1016/j.geomorph.2016.10.011.

722 Stolle, J., Takabatake, T., Nistor, I., Mikami, T., Nishizaki, S., Hamano, G., Ishii, H., Shibayama, T.,
723 Goseberg, N., & Petriu, E. (2018). Experimental investigation of debris damming loads under
724 transient supercritical flow conditions. *Coastal engineering*, 139, 16-31. doi:
725 10.1016/j.coastaleng.2018.04.026.

726 Takahashi, S., Sugano, T., Tomita, T., Arikawa, T., Tatsumi, D., Kashima, H., Murata, S., Matsuoka, Y., &
727 Nakamura, T. (2010). *Joint Survey for 2010 Chilean Earthquake and Tsunami Disaster in Ports
728 and Coasts* (PARI Technical Note 1224). Kuriyama, Japan: Port and Airport Research Institute.

729 Thieken, A. H., Bubeck, P., Heidenreich, A., von Keyserlingk, J., Dillenardt, L., & Otto, A. (2023).
730 Performance of the flood warning system in Germany in July 2021 – insights from affected
731 residents. *Nat. Hazards Earth Syst. Sci.*, 23(2), 973-990. doi: 10.5194/nhess-23-973-2023.

732 Waldner, P., Rickli, C., Köchli, D., Usbeck, T., Schmocker, L., & Sutter, F. (2007). Schwemholz. In G. R.
733 Bezzola & C. Hegg (Eds.), *Ereignisanalyse Hochwasser 2005, Teil 1 - Prozesse, Schäden und
734 erste Einordnung* (pp. 181-193). Bundesamt für Umwelt (BAFU),.

- 735 Wohl, E., Bledsoe, B. P., Fausch, K. D., Kramer, N., Bestgen, K. R., & Gooseff, M. N. (2016). Management
736 of large wood in streams: an overview and proposed framework for hazard evaluation. *JAWRA*
737 *Journal of the American Water Resources Association*, 52(2), 315-335.
- 738 Wüthrich, D., Arbós, C. Y., Pfister, M., & Schleiss, A. J. (2020). Effect of Debris Damming on Wave-
739 Induced Hydrodynamic Loads against Free-Standing Buildings with Openings. *Journal of*
740 *Waterway, Port, Coastal, and Ocean Engineering*, 146(1), 04019036. doi:
741 doi:10.1061/(ASCE)WW.1943-5460.0000541.
- 742 Wüthrich, D., Korswagen, P. A., Selvam, H., Oetjen, J., Bricker, J., & Schüttrumpf, H. (2024). Field survey
743 assessment of flood loads and related building damage from the July 2021 event in the Ahr
744 Valley (Germany). *Journal of Flood Risk Management*, e13024. doi: 10.1111/jfr3.13024.